Desalination and Water Treatment
www.deswater.com
1 (2009) 75–81
1944-3994/1944-3986

Studies on a water-based absorption heat transformer for desalination using MED

G. Srinivas, S. Sekar, R. Saravanan*, S. Renganarayanan

Institute for Energy Studies, Anna University, Chennai 600025, India
Tel. +91 44 2220 3268; email id: rsaravanan@annauniv.edu

Received 23 March 2007; Accepted 10 September 2008

ABSTRACT

Vapor absorption heat transformer coupled with MED system is an attractive option for water desalination using low temperature waste heat. A simulation model has been developed to predict the performance characteristics such as coefficient of performance (COP), distilled water output, total specific thermal energy consumption (OSTEC) and performance ratio (PR) of the coupled system for various water based working fluid combinations. For waste heat input in the temperature range of 60°C to 80°C and sink temperature in the range of 20°C to 40°, the performance of water based working fluids is compared, while considering gross temperature lift (GTL) up to 40°C. The results show that between the specified range of operating conditions, the working fluid system H_2O–($LiCl+LiNO_3$) gives the highest COP while consuming the lowest specific thermal energy for water purification using the coupled system, followed by H_2O–LiBr, H_2O–LiI, H_2O–($LiBr+LiNO_3$), H_2O–($LiBr+ZnBr_2+LiCl_2$) and H_2O-($LiCl+CaCl_2+Zn(NO_3)_2$) systems respectively. It is also found that a working fluid combination H_2O–$LiCl+CaCl_2+Zn(NO_3)_2$ produces the highest distilled water output compared to the other combinations. PR is the same for all working fluid combinations at given operating conditions and is found to increase with the number of effects (N) of MED.

Keywords: Water purification; Heat transformer; Water-based working fluids; Performance ratio

1. Introduction

The demand for good-quality water is continuously rising owing to the rise in the population, intense agricultural practices, industrialization and overall rise in living standards. In a majority of areas (near the seashore, industrial cluster) saline water needs to be treated for consumption. The most commonly applied desalination processes are multi-stage flash (MSF), multi-effect distillation (MED) with thermal vapor mompression (ME–TVC) or with mechanical vapor compression (ME–MVC) and reverse osmosis (RO). MED is most suitable for low-capacity systems compared to other methods [1]. Water purification using waste heat is a very attractive option due to depletion of fossil fuels and its associated emission issues. Among the different combinations of MED technologies available, the focus is on the multi-effect absorption heat pump system (ME–ABS) and the multi-effect adsorption heat pump system (ME–ADS) due to their capability to use waste heat for their operation.

Among the various methods of waste heat options available, the absorption heat transformer is a promising system since it consumes a small quantity of electrical energy or mechanical energy for its operation [2–4]. It delivers a part of the heat input at a higher temperature and the rest at a lower temperature. Waste heat or solar thermal energy can be used as heat input for a single-stage heat transformer while the high-grade thermal energy delivered by the heat transformer can be used as heat source for water desalination. A simulation model has been developed to determine the performance of an integrated vapor absorption heat transformer (VAHT) with MED for water purification using different water-based working fluid combinations.

*Corresponding author.

2.. Working principle of single-stage VAHT coupled with MED

A single-stage heat transformer consists of an evaporator, condenser, generator, absorber and a solution heat exchanger. A certain quantity of waste heat Q_{GE} is added at an intermediate temperature level (T_{GE}) called source heat temperature to the generator to vaporise the working fluid from the weak salt solution containing a low concentration of absorbent. The vaporized working fluid flows to the condenser delivering an amount of heat Q_{CO} at low temperature level (T_{CO}) called sink temperature. The liquid leaving the condenser is pumped to the evaporator where it is evaporated by using a quantity of waste heat Q_{EV} at source temperature (T_{EV}). The vaporized refrigerant then flows to the absorber where it is absorbed by the strong salt solution coming from the generator and delivers heat Q_{AB} at a usable temperature level (T_{AB}). The weak solution then returns to the generator for the internal heat recovery in a solution heat exchanger. The fraction of upgraded thermal energy output at the absorber is delivered to MED to evaporate a part of feed water supplied to the first stage of MED as shown in Fig. 1. The steam generated in the first cell from brine evaporation is condensed in the second cell producing more steam, which cascades to the third cell and so on.

3. Water-based working fluids

Water is an excellent refrigerant having low vapor pressure as desired in the present case, high latent heat and low viscosity. Lithium bromide and other similar salts are very good absorbents having high vapor pressures and low specific heat [5]. H_2O–LiBr pair is a commercially used working fluid mixture for present generation absorption heat transformers, but due to its corrosive nature and thermal instability above 130°C, some salt components may be added to improve the performance of the heat transformer by increasing the solubility of the aqueous LiBr solution over a wide range of operating conditions. Based on a number of components, working fluids are classified as binary, ternary and quaternary working fluids. The performance, operational characteristics and cost of a vapor absorption system are strongly dependent on the properties of the refrigerant, absorbent and other salt components of the mixture. The most important thermodynamic and thermophysical properties such as specific heat, heat of mixing, vapor pressure of refrigerant and absorbent, P-T-X , and h-T-X relationships are obtained from the experimental correlations determined by various investigators. Thirteen water-based working fluid combinations, which are suitable for vapor absorption systems, are given in the Table 1 along with references considered in this study [6–20].

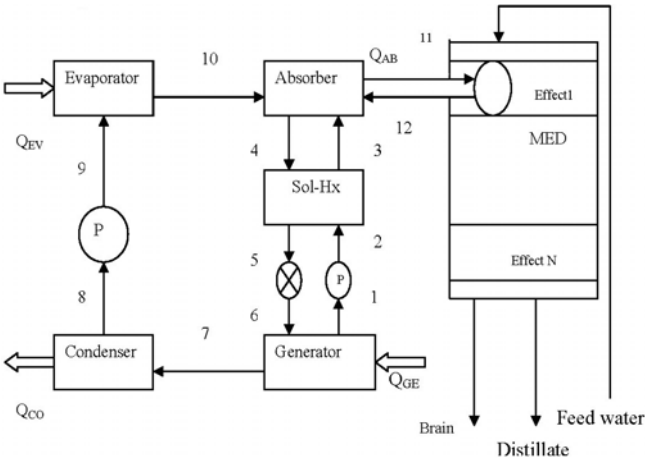

Fig. 1. Vapor absorption heat transformer coupled with MED for water purification.

Table 1
List of water-based working fluids along with property references

S. no	Combination (salt/mole ratio)	Property source
1	H_2O-LiBr	Herold et al., 1987 [6], Kumar, 1992 [7]
2	H_2O-LiI	Patil et al., 1991 [8]
3	H_2O-LiCl	Grover et al.,1988 [9]
4	H_2O-LiBr+LiI (4:1)	Iyoki et al., 1990 [10]
5	H_2O-LiCl+$LiNO_3$ (2.8:1)	Iyoki et al., 1993, [11]
6	H_2O-LiBr+$LiNO_3$ (4:1)	Iyoki, 1993 [12]
7	H_2O-LiBr+$ZnBr_2$ (2:1)	Adegoke et al., 1991 [13]
8	H_2O-LiBr+LiI+$C_2H_6O_2$ (3:1:1)	Iizuk et al, 1990 [14]
9	H_2O-LiBr+LiCl+$ZnCl_2$ (3:1:4)	Iyoki, 1993 [15]
10	H_2O-LiBr+$ZnCl_2$+$CaBr_2$ (1:1:0.13)	Iyoki et al., 1989 [16]
11	H_2O-LiBr+$ZnBr_2$+$LiCl_2$ (1:1.8:0.26)	Iyoki et al., 1990 [17]
12	H_2O-$LiNO_3$+KNO_3+$NaNO_3$ (53:28:19wt)	Ally, 1988 [18]
13	H_2O-LiCl+$CaCl_2$+$Zn(NO_3)_2$ (4.2:2.7:1)	Pinchuk et al., 1982 [19]
14	H_2O-LiBr+ $LiNO_3$LiI+LiCl (5:1:1:2)	Lee et.al, 2000 [20]

4. Methodology

The performance of the absorption heat transformer coupled with MED is evaluated from the following indices, considering the steady-state conditions and equal generator and evaporator temperatures.

1. Thermodynamic analysis is done by developing a mathematical model. The mathematical model for the absorption heat transformer is derived from the mass balance, concentration balance and energy balances around each component of VAHT. The general forms of the mathematical modeling equations are given below [21]:

$$\sum \dot{m}_i - \sum \dot{m}_o = 0 \tag{1}$$

$$\sum \dot{m}_I \times X_I - \sum \dot{m} \times X_O = 0 \tag{2}$$

$$\sum \dot{m}_i \times h_i - \sum \dot{m}_o \times h_o = 0 \tag{3}$$

$$X = f[T, P] \tag{4}$$

$$h = f[P, T, X] \tag{5}$$

2. Circulation ratio is determined from the mass flow rate of refrigerant and the weak solution flow rate, which are obtained from the Eqs. (1) and (2). It is defined as the ratio of the mass flow rate of solution coming from the absorber to the generator, to that of mass flow rate of the working fluid (refrigerant).

$$f = \frac{\dot{m}_W}{\dot{m}_R} = \frac{X_S}{X_S - X_W} \tag{6}$$

3. Concentration differential is defined as the percentage variation between strong and weak solution concentrations of the heat transformer. It determines the physical size of the absorber since it influences the mass transfer area. Strong solution concentration (X_S) and weak solution concentrations (X_W) can be obtained from Eq. (2) [22].

$$\mathrm{d}X = \frac{(X_S - X_W) \times 100}{X_S} \tag{7}$$

4. Temperature lift is defined as the temperature differential between the absorber temperature (T_H) and the heat source temperature(T_M).

$$GTL = T_{AB} - T_{GE} \tag{8}$$

5. Coefficient of performance (COP) is determined from the heat loads of absorber, generator and evaporator which are obtained from Eqs. (3) and (4). It is defined as the ratio absorber heat load (Q_{AB}) to the sum of the heat loads of generator (QGE) and evaporator (Q_{EV}) [23].

$$COP = Q_{AB} / [Q_{EV} + Q_{GE}] \tag{9}$$

6. Distilled water output of the MED unit is dependent on the number of effects (N) of MED, the quantity of thermal energy supplied by the absorber (Q_{AB}), latent heat of feed water and the absorber effectiveness. The distilled water flow rate is obtained approximately from the equation given below:

$$\dot{m}_D = Q_{AB} \times \varepsilon_{AB} \times (N-1) \times 3600 / (hfg \times 1000) \tag{10}$$

7. The quantity of total waste input required for the integrated system to produce 1 m^3/h of distilled water output is obtained from Eq. (11) as given below. OSTEC is the ratio of the sum of the evaporator and generator heat loads of VAHT to the distilled water flow output of MED unit.

$$OSTEC = \frac{Q_{EV} + Q_{GE}}{\dot{m}_D} \tag{11}$$

8. Performance ratio is an important characteristic of MED plants, which is calculated from the following equation [24]:

$$PR = \text{[Distillate flow rate (kg/s)} \times 2300 \text{ (kJ/kg)]} \text{ /heat input in the first effect (kW)} \tag{12}$$

5. Results and discussion

The selection of a suitable working fluid is desirable for water desalination using vapor absorption heat transformer coupled with MED since the performance of VAHT is dependant on the nature of working fluids. Selection criteria may be either a high COP or a high distilled water output flow rate. Simulation has been carried out for a fixed weak solution flow rate of 1 kg/s as a standard parameter in order to compare the performance of various water-based working fluid systems. The sink temperature (T_{CO}) is varied in the temperature range of 20°C to 40°C; the source heat temperature (T_{GE}=T_{EV}) is varied between 60°C and 80°C, while the gross temperature lift from 10°C to 30°C is considered to reflect the actual working conditions of heat transformer.

In Fig. 2, the effect of GTL between 10°C to 30°C is presented in terms of the COP of 13 water-based working fluid combinations, while keeping the generator temperature and condenser temperature at 60°C and 30°C respectively. Fig. 2 shows that the H_2O–($LiCl+LiNO_3$) system

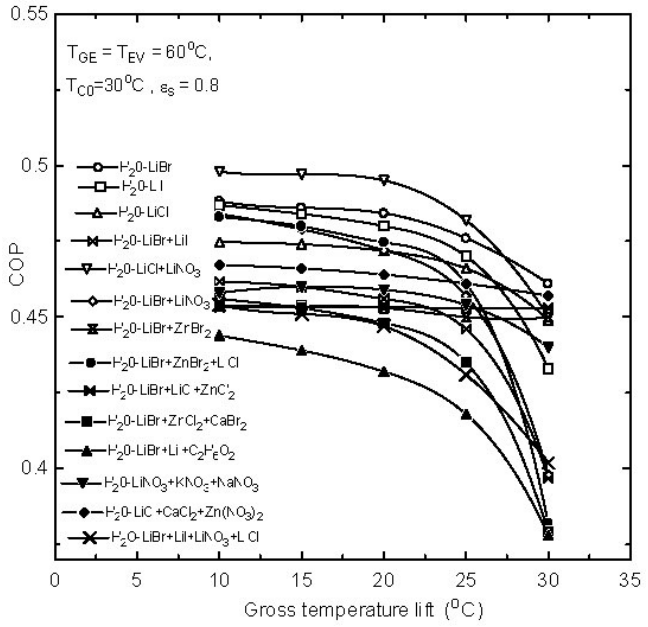

Fig. 2. Effect of GTL on COP.

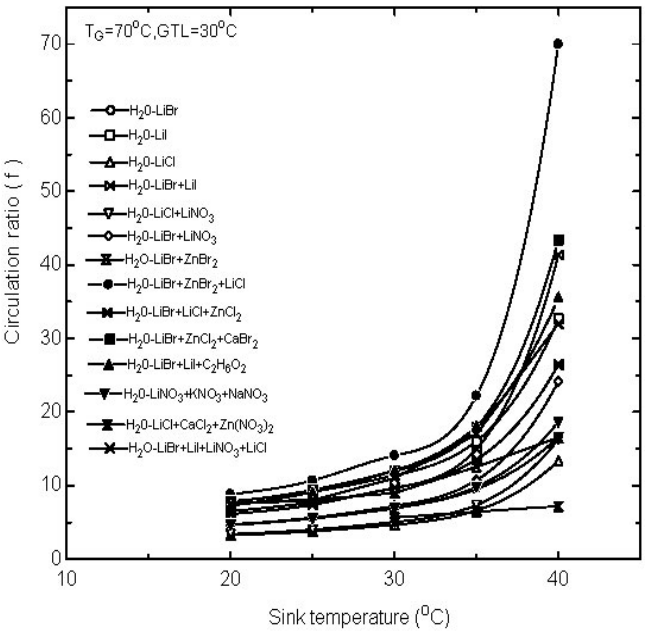

Fig. 3. Effect of GTL on circulation ratio (f).

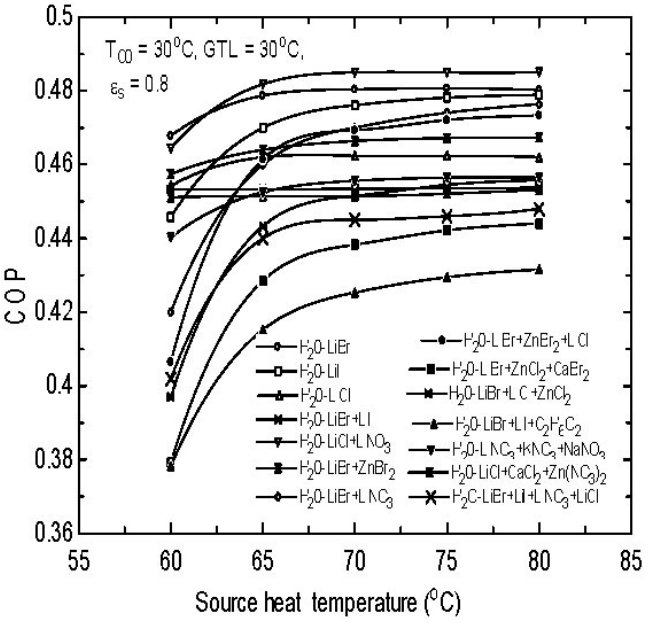

Fig. 4. Effect of source heat temperature on COP.

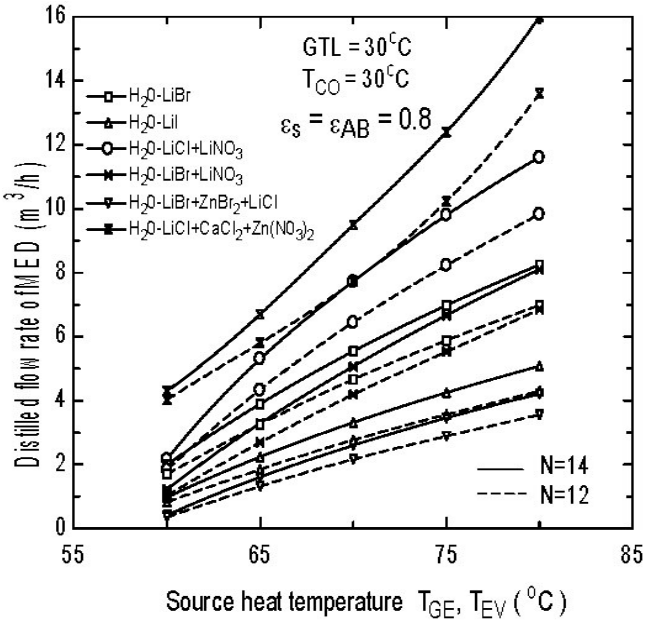

Fig. 5. Effect of Source heat temperature on distilled water output flow rate of MED.

gives the highest COP than other working fluids and COP decreases from 0.506 to 0.4599 as GTL is raised from 10°C to 40°C, at a solution heat exchanger effectiveness of 0.80. The COP of other working fluids combinations also show the same trend with respect to GTL. It is found that the working fluid systems H_2O–LiBr, H_2O–LiI, H_2O–($LiBr+LiNO_3$), H_2O–($LiBr+ZnBr_2+LiCl_2$) and H_2O–($LiCl+CaCl_2+Zn(NO_3)_2$) give the highest COP in decreasing order respectively next to the H_2O–($LiCl+LiNO_3$) system. This is because for any working fluid combination, the COP is higher for the system having a lower circulation ratio, as illustrated in Fig. 3. It shows the variation of the circulation ratio with respect to sink temperature. A circulation ratio of H_2O–($LiCl+LiNO_3$) and H_2O–($LiCl+CaCl_2+Zn(NO_3)_2$) systems is less than other working fluid systems over a given range of operating temperatures.

The effect of source heat temperature on COP is plotted in Fig. 4. Both GTL and condenser temperatures

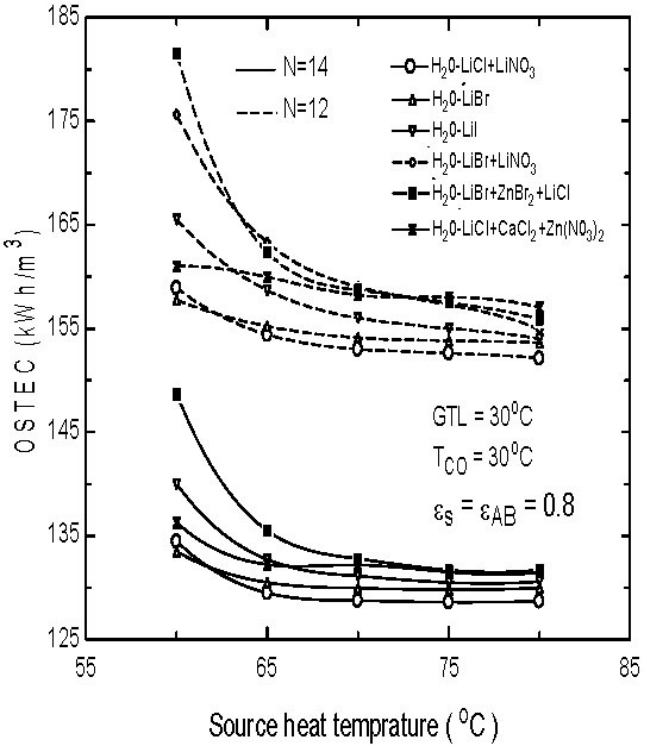

Fig. 6. Effect of Source heat temperature on total specific thermal energy consumption.

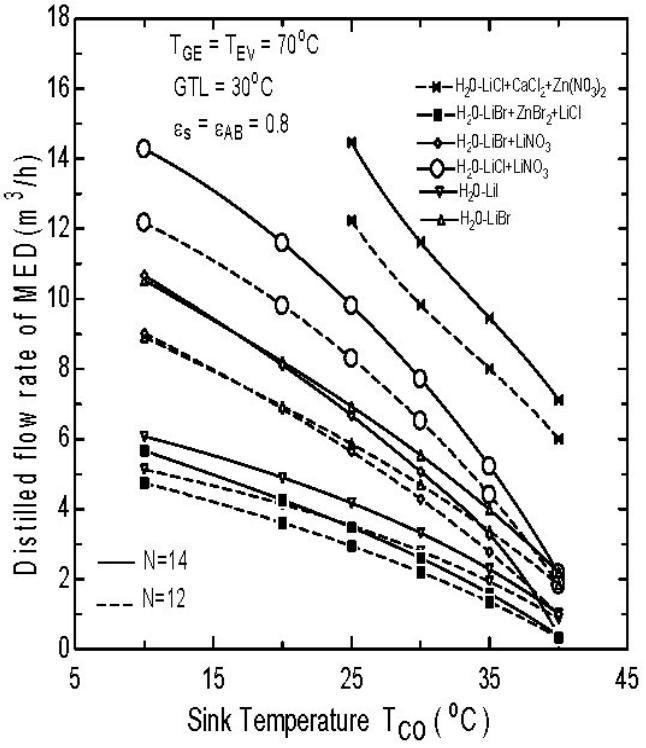

Fig. 7. Effect of condenser temperature on Distilled water flow rate of MED.

are kept at 30°C and solution heat exchanger effectiveness is fixed at 0.8. The COP of all working fluid combinations increases, as source heat temperature increases from 60°C to 80°C. The COP of the H_2O–($LiCl+LiNO_3$) combination increases from 0.464 to 0.485 and the COP of the H_2O–LiBr system increases from 0.467 to 0.48 as the source heat temperature rises from 60°C to 80°. It is found that the working fluid system H_2O–LiBr+LiI+$C_2H_6O_2$ has a lower COP than other working fluid combinations. The major variation of COP is produced between 60°C to 70°C and the variation is almost negligible between 70°C and 80°C.

The best six working fluid combinations giving the highest COP are considered for the integrated system of VAHT and MED for desalination. Top brain temperature (TBT) of MED is kept at 70°C. The effect of source heat temperature on distilled water output flow rate of MED unit is shown in Fig. 5 at a given solution heat exchanger effectiveness and absorber effectiveness of 0.8. Both condenser temperature and GTL are fixed at 30°C. For the given operating temperatures, distilled water output values are obtained for MED in 12 and 14 effects in order to compare the distilled water output of same working fluid combination at different number of effects. H_2O–($LiCl+CaCl_2+Zn(NO_3)_2$) is found to produce the highest distilled water output of 16 m^3/h at a source heat temperature of 80°C and distilled water output decreases to 4.1 m^3/h as the source heat temperature decreases to 60°C. The H_2O–($LiCl+LiNO_3$) and H_2O–LiBr systems produce 11.61 m^3/h and 8.25 m^3/h of distilled water respectively at 80°C. The working fluid combinations H_2O–($LiCl+LiNO_3$), H_2O–LiBr, H_2O–($LiBr+LiNO_3$), H_2O–LiI and H_2O–($LiBr+ZnBr_2+LiCl_2$) produce a quantity of distilled water in the decreasing order respectively next to H_2O–($LiCl+CaCl_2+Zn(NO_3)_2$).

The variation of overall specific thermal energy consumption for water purification with respect to source heat temperature is shown in Fig. 6. The condenser temperature and GTL are fixed at 30°C.For a given solution heat exchanger effectiveness and absorber effectiveness of 0.8, the overall specific thermal energy consumption (OSTEC) for water purification decreases as source heat temperature increases from 60°C to 80°C. Working fluid combinations H_2O–($LiCl+LiNO_3$) and H_2O–LiBr consume the least quantity of thermal energy for water purification respectively, while the H_2O–($LiBr+ZnBr_2+LiCl_2$) system consumes more thermal energy than other working fluid systems. OSTEC is obtained for MED having 12 and 14 effects, and it is also shown that for a particular working fluid system the overall specific energy consumption for water purification increases as the number of effects of MED unit decreases.

Fig. 7 shows the effect of sink temperature in terms of distilled water output flow rate. Condenser temperature is varied between 10°C to 40°C, while keeping the generator

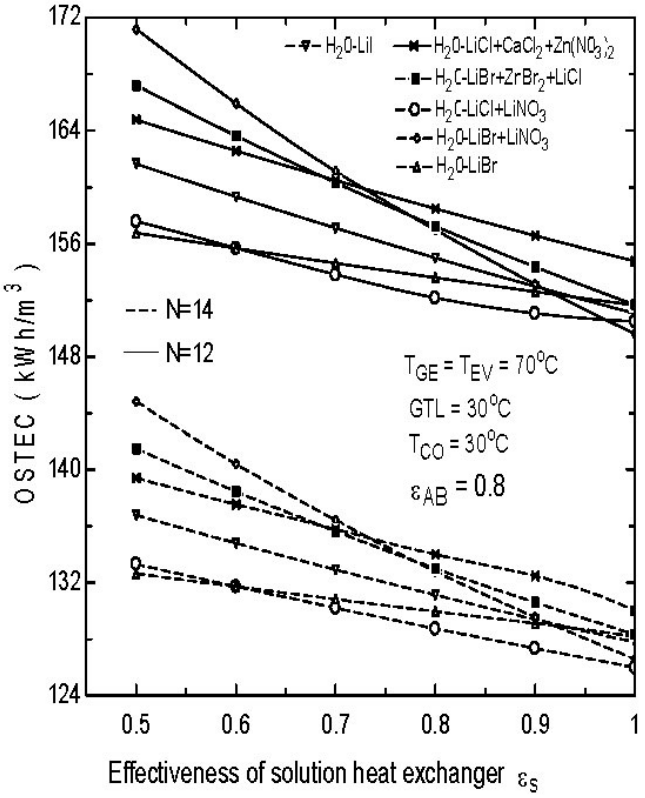

Fig. 8. Effect of Solution heat exchanger effectiveness on overall specific thermal energy consumption.

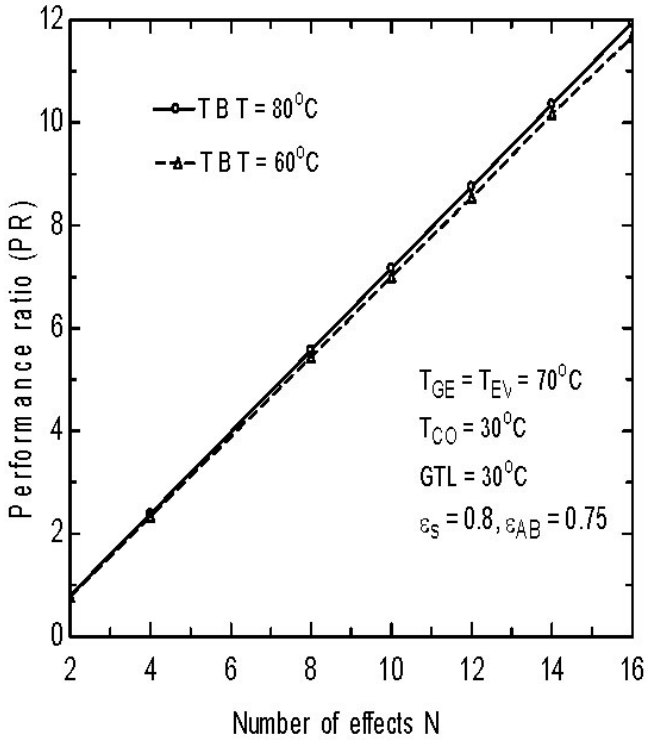

Fig. 9. Effect of number of effects on performance ratio of MED.

temperature and GTL at 70°C and 30°C respectively. The distilled water output flow rate decreases as condenser temperature increases from 10°C to 40°C.For a given solution heat exchanger effectiveness and absorber effectiveness of 0.8, H_2O-(LiCl+$CaCl_2$+Zn $(NO_3)_2$) system is found to produce the highest distilled water output followed by H_2O-(LiCl+$LiNO_3$) ,H_2O-LiBr and H_2O-(LiCl+$LiNO_3$) systems respectively .

The influence of solution heat exchanger effectiveness on overall specific energy consumption is shown in Fig. 8. At generator and condenser temperatures of 70°C and 30°C respectively, the effectiveness of the solution heat exchanger is varied from 0.5 to 1 while keeping GTL at 30°C. OSTEC for water purification decreases as the effectiveness of the solution heat exchanger increases. The working fluid system H_2O–(LiBr+$LiNO_3$) is found to consume the highest specific thermal energy for water purification between a solution heat exchanger effectiveness of 0.5 and 0.7. For a solution heat exchanger effectiveness between 0.7 and 1, the H_2O–(LiCl+$CaCl_2$+Zn $(NO_3)_2$) system is found to consume more OSTEC than other combinations. For MED with 14 effects, the OSTEC of the H_2O–(LiBr+$LiNO_3$) system decreases from 171.16 kWh/m^3 to 153.1 kWh/m^3 as the effectiveness of the solution heat exchanger increases from 0.5 to 1. The working fluid system H_2O–(LiCl+$LiNO_3$) consumes less thermal energy for water purification than other working fluid combinations throughout the specified range of effectiveness. For MED with 14 effects, the OSTEC of H_2O–(LiCl+$LiNO_3$) system varies from 133.4 kWh/m^3 to 127.4 kWh/m^3 as the effectiveness of the solution heat exchanger increases from 0.5 to 1.

The effect of the number of effects of MED on PR is presented in Fig. 9. The number of effects is varied from 2 to 16, and the PR of the MED plant is determined for a TBT of 60 to 80°C. It is found that all working fluids have the same PR for a given number of effects and at chosen operating temperatures of the coupled system. It is also found that PR is proportional to the number of effects of a MED plant and the effect of TBT on PR is negligible as indicated in the figure.

6. Conclusions

The distilled water output flow rate (m^3/h) of MED and total specific thermal energy consumption (kWh/m^3) of coupled systems were determined for various working fluid combinations at different operating conditions and effectiveness of the solution heat exchanger in order to identify the most suitable water-based working fluid systems giving the highest COP, distilled water flow,

while consuming less specific thermal energy for water purification. The working fluid giving the highest COP may not produce the greatest quantity of distilled water.

Among the results specified, the H_2O–(LiCl+$LiNO_3$) achieved the highest COP of 0.506. The H_2O–(LiCl+$CaCl_2$+Zn $(NO_3)_2$) system produced the highest distilled water output of 16 m^3/h, while having an OSTEC of 134 kWh/m^3. For the integrated system having 14 effects, thermal energy required for 1 m^3/h of distillate output is around 120 to 150 kW over a wide range of operating temperatures. From an energy point of view, it is desirable to have a higher number of effects in MED, since specific energy consumption required for water purification decreases and the PR of a MED plant increases with the number of effects.

7. Symbols

f — Circulation ratio
h — Enthalpy, J kg^{-1}
hfg — Latent heat evaporation of water, J kg^{-1}
$\dot{m}$ — Mass flow rate, kg s^{-1}
P — Pressure, kPa
Q — Heat load, kW
T — Temperature, °C
X — Concentration, %
dX — Concentration differential, %
ε — Effectiveness of solution heat exchanger

Subscripts

AB — Absorber
CO — Condenser
D — Distillate
EV — Evaporator
GE — Generator
i — Inlet
o — Outlet
R — Refrigerant
S — Strong solution
s — Solution heat exchanger
W — Weak solution
1...12— Number of state points of the cycle shown in Fig. 1

Acknowledgement

The financial support received from the University Grants Commission (UGC), New Delhi, Government of India, is gratefully acknowledged.

References

[1] M. Al-Shammiri and M. Safar, Multi-effect distillation plants: state of the art. Desalination, 126 (1999) 45–59.
[2] A. Huicochea, J. Siqueiros and R.J. Romero, Portable water purification system integrated to a heat transformer. Desalination, 165 (2004) 385–391.
[3] R. Saari, Usability of low temperature waste heat for sea water desalination. Desalination, 39 (1981) 147–158.
[4] J. Siqueiros and R.J. Romero, Increase of COP for heat transformer in water purification systems. Part I—Increasing heat source temperature, Appl. Thermal Eng., 27 (2007) 1043–1053.
[5] R. Saravanan, Studies on two-fluid bubble pump operated vapor absorption refrigeration system, PhD Thesis, IIT Madras, Chennai, 1999.
[6] K.E. Herold and M.J. Morjan, Thermodynamic properties of lithium bromide/water solution, Part 1, ASHRAE Trans., 93 (1987) 35–48.
[7] A. Kumar and V. S. Patwardhan, Vapor pressure and enthalpy of aqueous lithium bromide solutions. Heat Rec. Sys. CHP, 12(4) (1992) 311–315.
[8] K.R. Patil, S.K. Chaudhari and S.S. Katti, Thermodynamic design data for absorption heat transformers, Part III, Operating on water-lithium iodide, Heat Rec. Sys. CHP, 11(5) (1991) 361–369.
[9] G.S. Grover, S. Devotta and F.A. Holland, Thermodynamic design data for absorption heat transformers, Part III. Operating on water-lithium chloride. Heat Rec. Sys. CHP, 8(5) (1988) 425–431.
[10] S. Iyoki, S. Ohemori and T. Uemura, Heat capacities of water–lithium bromide–lithium iodide system. J. Chem. Eng. Data., 35 (1990) 317–320.
[11] S. Iyoki, Y. Kuriyama and T. Uemura, Vapor pressures of water–lithium chloride–lithium nitrate system. J. Chem. Thermodyn., 25 (1993) 569–577.
[12] S. Iyoki, R. Yamanaka and T. Uemura, Physical and thermal properties of the water–lithium bromide–lithium nitrate system, Int. J. Refrig., 16 (1993) 191–200.
13] C.O. Adegoke and W.B. Gosney, Vapor pressure data for LiBr+$ZnBr_2$–H_2O solutions, Int. J. Refrig., 16 (1991) 39–45.
[14] H. Iizuka and K. Nagamatsuya, New working fluids containing ethylene-glycol for air-cooled chillers, 2. Proc. 3rd International Energy Agency Heat Pump Conference, Tokyo, 1990, pp. 565–574.
[15] S. Iyoki, Water–lithium bromide+lithium chloride zinc chloride system, Refrig., 68 (1993) 46–49.
[16] S. Iyoki and T. Uemura, Performance characteristics of the water–lithium bromide–zinc chloride–calcium bromide absorption refrigerating machine. Absorption heat pump and absorption heat transformer, Int. J. Refrig., 12 (1989) 272–277.
[17] S. Iyoki and T. Uemura, Physical and thermal properties of the water–lithium bromide–zinc bromide–lithium chloride system, Part 2, ASHRAE Trans., 96 (1990) 323–328.
[18] M.R. Ally, Vapour liquid equilibrium and enthalpy concentration temperature correlations for ternary nitrate mixtures, Part 2, ASHRAE Trans., 94 (1988) 631–638.
[19] O.A. Pinchuk, I.I. Orekhov and S.V. Karavan, Investigation of thermodynamic properties of multi-component solution for absorption refrigerating machine, Kholodinana Tekhnik, 6 (1982) 36–38.
[20] H.R. Lee, K.-K. Koo, S. Jeong, J.-S. Kim, H. Lee, Y.-S. Oh, D.-R. Park and Y.-S. Baek, Thermodynamic design data and performance evaluation of the water + lithium bromide + lithium iodide + lithium nitrate + lithium chloride system for absorption chiller. Appl. Eng., 20 (2000) 707–720.
[21] J. Yin, L. Shi, M.-S. Zhu and L. Zhong, Performance analysis of an absorption heat transformer with different working fluid combinations, Appl. Energy, 67(3) (2000) 281–292.
[22] M. Bourouis, A. Coronas, R.J. Romero and J. Siqueiro, Purification of seawater using absorption heat transformers with water–(LiBr+LiI+LiNO3+LiC1) and low temperature heat sources, Desalination, 166 (2004) 209–214.
[23] A. Jernqvist, K. Abrahamsson and G. Aly, On the efficiencies of absorption heat transformers, Heat Rec. Sys. CHP, 12(4) (1992) 323–334.
[24] A. Hatzikioseyian, R. Vidali and P. Kousi, Modelling and thermodynamic analysis of a multi effect distillation (MED) plant for seawater desalination, http//www.metal.ntua.gr/uploads/3024/179.